Binder Jetting Additive Manufacturing: The Effect of Feed Region Density on Resultant Densities

Quinton Porter
Department of Mechanical Engineering,
Texas A&M University,
College Station, TX 77843
e-mail: kuqjp000@tamu.edu

Ming Li
Department of Industrial and Systems Engineering,
Texas A&M University,
College Station, TX 77843
e-mail: xaviorsbear2015@tamu.edu

Zhijian Pei
Department of Industrial and Systems Engineering,
Texas A&M University,
College Station, TX 77843
e-mail: zjpei@tamu.edu

Chao Ma[1]
Department of Mechanical Engineering,
Texas A&M University,
College Station, TX 77843;
Department of Industrial and Systems Engineering,
Texas A&M University,
College Station, TX 77843;
Department of Engineering Technology and Industrial Distribution,
Texas A&M University,
College Station, TX 77843
e-mail: cma@tamu.edu

This technical brief reports an experimental investigation on the effect of feed region density on resultant sintered density and intermediate densities (powder bed density and green density) during the binder jetting additive manufacturing process. The feed region density was increased through compaction. The powder bed density and green density were determined by measuring the mass and dimension. The sintered density was measured with the Archimedes' method. As the relative feed region density increased from 44% to 65%, the powder bed density increased by 5.7%, green density by 8.5%, and finally sintered density by 4.5%. Statistical testing showed that these effects were significant. This study showed that compacting the powder in the feed region is an effective method to alter the density of parts made via binder jetting additive manufacturing. [DOI: 10.1115/1.4054453]

Keywords: additive manufacturing, binder jetting, alumina, feed region, density, compaction

1 Introduction

Many applications such as tooling and biomedical implants can benefit from binder jetting (BJ) additive manufacturing. A wide range of researchers have reported their studies on BJ [1–13]. Many published studies are on how final density (usually the sintered density) in the BJ process is affected [4–13].

A common method for altering the final density is to alter the intermediate densities (powder bed density and green density) [4,5]. The work by Li et al. indicated that the powder bed density approximately equaled feed region density [13]. According to this result, a natural conjecture is that increasing the feed region density (e.g., by compacting the powder in the feed region) might increase the powder bed density (and consequently green density and final density). In fact, some 3D printer manufacturers suggest that operators should compact the powder in the feed region to improve the final density. However, the literature does not have experimental data to substantiate the conjecture. It is not clear how powder spreading affects this conjecture because the spreader (roller or blade) disrupts the original particle packing and rearranges the particles when it moves the powder from the feed region to the build region (in which the powder bed is located). The previous work by Li et al. [13] was conducted without any compaction; therefore, it is still unknown how increasing the feed region density affects the final density and the intermediate densities (powder bed density and green density), especially considering the particle rearrangement during powder spreading.

This study aims to experimentally determine whether compacting the powder in the feed region can result in a corresponding increase in the powder bed density, green density, and final density (sintered density). The experiments were carried out on a commercially available BJ 3D printer. Statistical testing was conducted on the experimental data.

2 Materials and Methods

2.1 Powder Characterization. This study was conducted on alumina powder with a nominal particle size of 20 μm provided by Inframat. A laser scattering machine (HORIBA LA-960) was used to measure the particle size distribution of the alumina powder, which was repeated thrice. A scanning electron microscope (SEM; JEOL JSM-7500F) was used to characterize the morphology of the alumina powder.

2.2 Binder Jetting. A commercially available BJ 3D printer (ComeTrue T10, Microjet Technology) was used for conducting experiments. To reduce the amount of powder needed for the experiments, two sets of custom devices, which were created in the previous work [13], were installed on the 3D printer. Figure 1 depicts how the two custom inserts were placed above the original feed region platform and the original build region platform of the 3D printer and aligned with the top of the feed region and the build region. The two custom pistons with a size of 25×25 mm^2 for the feed region and build region were fixed to the original platforms, which allowed the custom pistons to follow the downward and upward movements of the original platforms during the printing process.

A Hall funnel was used in each BJ trial to consistently add powder into the feed region. An 88 mm gap was maintained between the base of the Hall funnel and the base of the feed region. To measure the initial feed region density without compaction, the powder was flowed from the Hall funnel until it filled the feed region, and a slide was used to create a flat upper surface. A caliper with a resolution of 0.01 mm was used to measure the height of each of the four corners of the powder in the feed region. The average was used to calculate the volume within the known area of the feed region. The mass of the powder was measured with a balance scale having a 0.001 g resolution. The relative feed region density, ρ'_{fr}, was calculated using Eq. (1):

$$\rho'_{fr} = \frac{m_{fr}}{h_{fr} A_{fr} \rho_{th}} \tag{1}$$

[1]Corresponding author.

Manuscript received December 13, 2021; final manuscript received April 21, 2022; published online May 19, 2022. Assoc. Editor: Ran Jin.

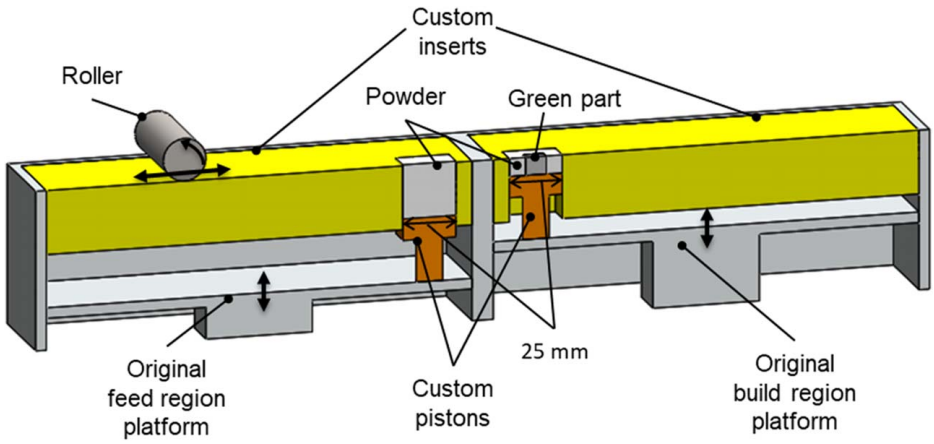

Fig. 1 A graphic illustration showing the cross section of the custom pistons and inserts on the 3D printer

where A_{fr} is the area of the feed region, h_{fr} is the average height of the powder in the feed region, m_{fr} is the mass of the powder in the feed region, and ρ_{th} is the theoretical density of the material (alumina in this study), which is 3.97 g/cm^3. A relative feed region density of 44% was obtained without compaction, and 55% and 65% were chosen as the other two feed region densities to investigate. To achieve a relative feed region density of either 55% or 65%, a predetermined amount (45 g) of powder was flowed into the feed region from the Hall funnel. This amount was selected because it was enough to complete the designed printing experiments. After filling the feed region with powder, a mechanical stop was placed over the opening of the feed region, and the base was raised to reduce the volume to the appropriate size. It is noteworthy to mention that this technique is applicable to other commercially available 3D printers without the need of incorporating the custom devices. After the feed region was prepared, the printing process followed in accordance with the parameters presented in Table 1. The dosing ratio is the amount of the powder provided from the feed region compared to the amount of powder needed to fill a layer on the powder bed. A dosing ratio of 1.4 ensured that enough powder was present to completely form that layer. The printing time determines how many times the printhead scans the cross section and thus controls the binder saturation. A print time of 1 resulted in green specimens with sufficient strength for handling. Each print had four specimens, and two prints were done at each feed region density. Eight specimens at each feed region density were cured for 2 h at 35 °C. Green specimens were then obtained after removing the loose powder surrounding them.

2.3 Debinding and Sintering. The specimens were debound and sintered with the following process: heating from room temperature to 500 °C at 3.2 °C/min, heating from 500 °C to 1150 °C at 2.4 °C/min, heating from 1150 °C to 1700 °C at 0.8 °C/min, dwelling at 1700 °C for 120 min, and finally cooling in the furnace to room temperature via natural convection. They were then removed from the furnace for investigation.

Table 1 Printing parameters for the BJ process

Printing parameter	Value
Dosing ratio	1.4
Printing time	1
Layer thickness (mm)	0.16
Roller traverse speed (mm/s)	50
Roller rotation speed (rpm)	500

2.4 Density Measurement. To measure the powder bed density, powder spreading was conducted for 50 layers using the same setup described in Sec. 2.1. The spreading parameters were the same as those used for printing, as listed in Table 1. After finishing powder spreading, excess powder in the space between the roller and the custom inserts on the build platform was removed. The heights of the powder in the build region at four corners were measured using the same caliper as described in Sec. 2.2. The powder was then collected to measure the mass using the same balance scale as described in Sec. 2.2. The powder bed density, ρ_{pb}, was then calculated using Eq. (2):

$$\rho_{pb} = \frac{m_{pb}}{h_{pb} A_{pb}} \tag{2}$$

where A_{pb} is the area of the build region, m_{pb} is the mass of the powder in the build region, and h_{pb} is the average height of the powder in the build region. Powder spreading was conducted three times at each feed region density to measure the powder bed density.

The green specimens were dimensionally measured with a caliper to obtain the green density, ρ_g, using Eq. (3):

$$\rho_g = \frac{m_g}{h_g l_g w_g} \tag{3}$$

where m_g is the mass, h_g is the height, l_g is the length, and w_g is the width.

Sintered density was measured using Archimedes' principle in Eq. (4) to obtain the bulk density [14]:

$$\rho_s = \frac{\rho_w m_d}{m_w - m_s} \tag{4}$$

where ρ_s is the bulk density of the sintered specimen, ρ_w is the density of the water, m_d is the dry mass, m_w is the wet mass, and m_s is the submerged mass.

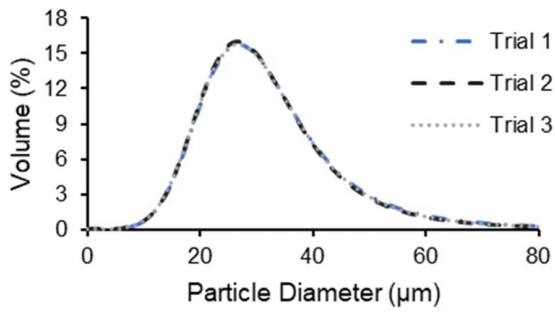

Fig. 2 Particle size distribution of the alumina powder

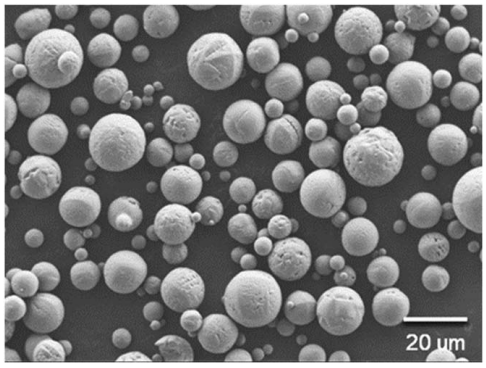

Fig. 3 Scanning electron micrograph of the alumina powder

The resulting density data were then put through a statistical analysis to determine whether there are significant effects of feed region density on powder bed density, green density, and sintered density.

2.5 Microscopy. The sintered specimens were mechanically fractured to reveal the interior surface for microscopy. Specimens were imaged with the TESCON VEGA II LSU SEM.

3 Results and Discussion

3.1 Powder Size and Morphology. Figure 2 presents the three trials for the particle size distribution measurement of the alumina powder with the laser scattering machine. The mean size is 26.4 μm with a median of 24.8 μm, so the particles are slightly larger than the nominal size of 20 μm on average.

The morphology of the powder is shown in Fig. 3. The particles are largely spherical and do not appear to agglomerate. The lack of agglomerations indicates higher likelihood for good spreadability.

3.2 Density. Figure 4 shows the measured powder bed density, green density, and sintered density as a function of feed region density. An increasing trend is captured and depicted for each phase of the BJ process. A higher feed region density correlates with a higher powder bed density, green density, and sintered density.

To determine whether feed region density has a statistically significant effect on powder bed density, green density, and sintered density, three analysis of variance tests were conducted. The sample size was three for analyzing the powder bed density at each feed region density. For the green density and sintered density analysis, the sample size was eight at the feed region density of 44% and was seven at the feed region densities of 55% and 65% because of one of the eight specimens was damaged in these two cases. The p-values are 0.0015, 0.0009, and 0.0002 for powder bed density, green density, and sintered density, respectively. The small p-values are far lower than the commonly accepted significance level of 0.05 for the three tests, verifying that the feed region density has a significant effect on each of the three investigated phases of the BJ process.

Given the information earlier, a post hoc t-test was used to determine whether there is a significant difference in each investigated phase between all three feed region densities as shown in Eq. (5):

$$t = \frac{\bar{Y}_1 - \bar{Y}_2}{\sqrt{\frac{s_1^2}{N_1} + \frac{s_2^2}{N_2}}} \tag{5}$$

where $\bar{Y}$ is the mean of the sample set, s is the standard deviation, and N is the sample size.

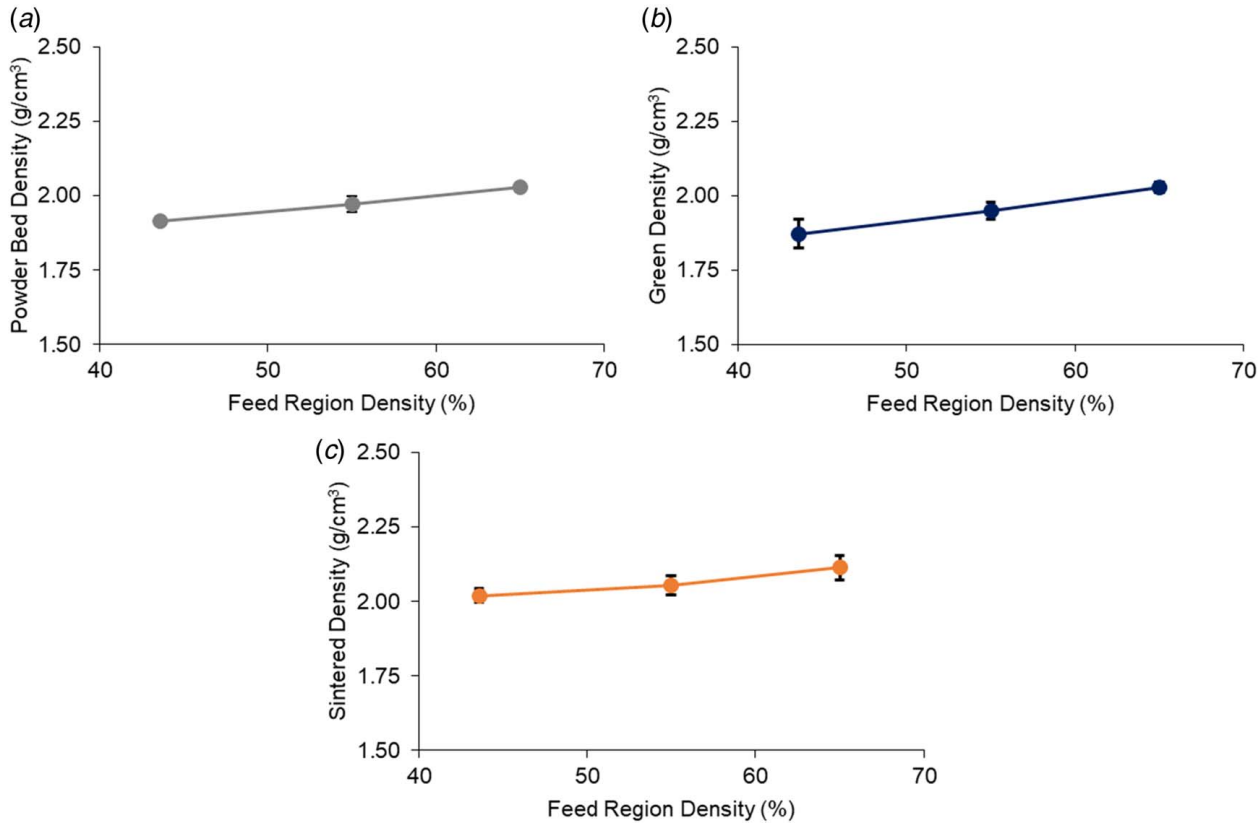

Fig. 4 The effect of feed region density on (*a*) powder bed density, (*b*) green density, and (c) sintered density for the alumina powder

Table 2 Powder bed density data

Feed region density (%)	Mean powder bed density (g/cm^3)	Standard deviation of powder bed density (g/cm^3)	Sample size
44	1.92	0.02	3
55	1.97	0.03	3
65	2.03	0.02	3

Table 3 Green density data

Feed region density (%)	Mean green density (g/cm^3)	Standard deviation of green density (g/cm^3)	Sample size
44	1.87	0.05	8
55	1.95	0.03	7
65	2.03	0.02	7

Table 4 Sintered density data

Feed region density (%)	Mean sintered density (g/cm^3)	Standard deviation of sintered density (g/cm^3)	Sample size
44	2.02	0.02	8
55	2.05	0.03	7
65	2.11	0.04	7

The mean powder bed densities for the three investigated feed region densities, 44%, 55%, and 65%, were compared with the data provided in Table 2. The p-values for the comparison of 44% and 55%, 55% and 65%, and 44% and 65% are 0.038, 0.034, and 0.001, respectively. The p-values being lower than 0.05 validates that mean powder bed densities are statistically different from one another with greater than 95% confidence.

The mean green densities for the three investigated feed region densities, 44%, 55%, and 65%, were compared with the data provided in Table 3. The p-values for the comparison of 44% and 55%, 55% and 65%, and 44% and 65% are 0.015, 0.012, and 0.003, respectively. The p-values being lower than 0.05 validates that the mean green densities are statistically different from one another with greater than 95% confidence.

The mean sintered densities for the three investigated feed region densities, 44%, 55%, and 65%, were compared with the data provided in Table 4. The p-values for the comparison of 44% and 55%, 55% and 65%, and 44% and 65% are 0.048, 0.017, and 0.0002, respectively. The p-values being lower than 0.05 validates that the mean sintered densities are statistically different from one another with greater than 95% confidence.

The powder bed density was increased by 5.7%, the green density was increased by 8.5%, and the sintered density was increased by 4.5% as a result of increasing the feed region density from 44% to 65%. The likely reason for this increase in these densities is the increase in the effective dosing ratio. By compacting the feed region, more powder is made available for the spreading of each layer without increasing the layer height although the nominal dosing ratio is the same. However, the future work is required to confirm or reject this likely reason.

3.3 Microstructure. Figure 5 shows the fracture surfaces of the sintered specimens at three different magnifications. All the sintered specimens show a low amount of necking and clear granular structures. This is mainly because of the large particle size and thus the low sinterability of the powder. The different densities at various feed region densities are difficult to identify visually, but the third row of Fig. 5 (at the highest density in this study) shows slightly denser packing of the sintered particles.

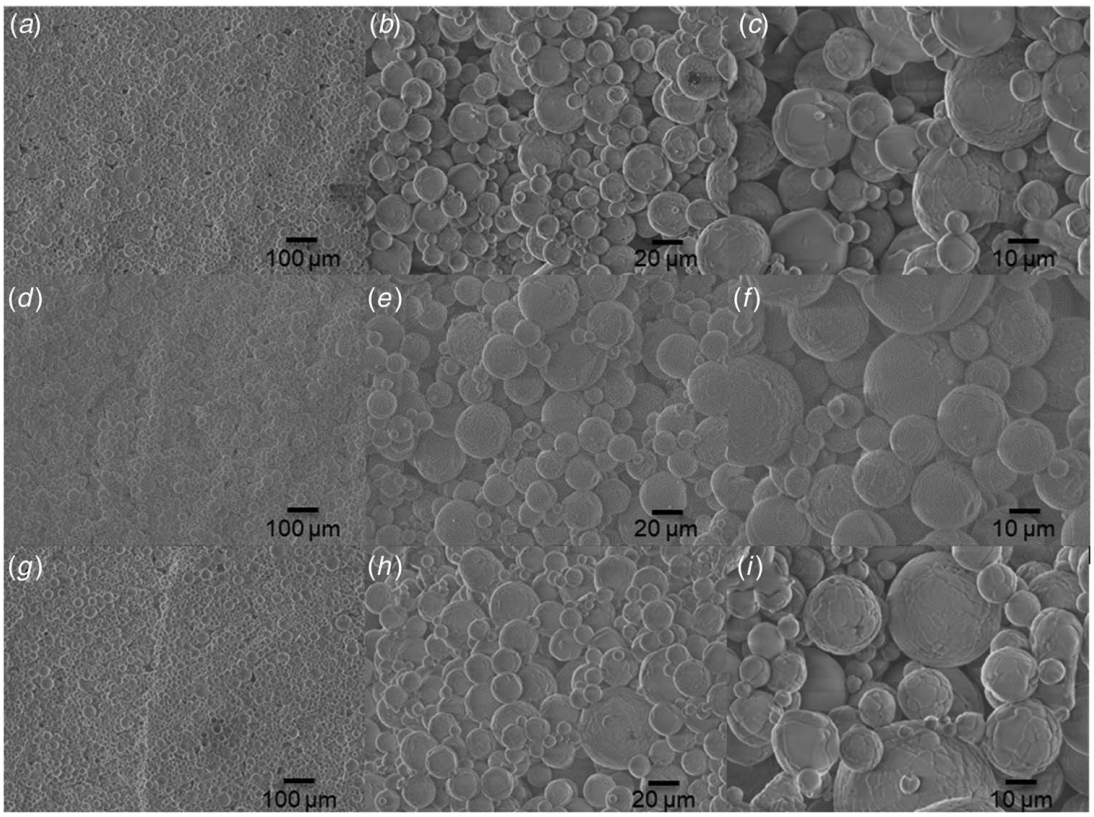

Fig. 5 The fracture surface of the sintered specimens at various feed region densities: (*a–c*) 44%, (*d–f*) 55%, and (*g–i*) 65%

4 Conclusions

This experimental investigation into the effects of feed region density on the density of the powder beds, green specimens, and sintered specimens showed that they were significant. A higher density in the feed region resulted in a higher density for the specimens throughout the BJ process. The statistical testing verified that the differences in the mean powder bed density, green density, and sintered density were significant with greater than 95% confidence. By increasing the relative feed region densities from 44% to 65%, the powder bed density, green density, and sintered density was increased by 5.7%, 8.5%, and 4.5%, respectively. Compacting the powder in the feed region before printing can alter the sintered density of the product produced by BJ. This can be beneficial for various applications where density plays an important role, such as tooling and biomedical implants.

Funding Data

- National Science Foundation (Grant No. 2047908).

Conflict of Interest

There are no conflicts of interest.

Data Availability Statement

The authors attest that all data for this study are included in the paper.

Declaration of Competing Interest

The authors declare that they have no known competing financial interests or personal relationships that could have appeared to influence the work reported in this paper.

References

[1] Ziaee, M., and Crane, N. B., 2019, "Binder Jetting: A Review of Process, Materials, and Methods," Addit. Manuf., **28**, pp. 781–801.

[2] Lv, X., Ye, F., Cheng, L., Fan, S., and Liu, Y., 2019, "Binder Jetting of Ceramics: Powders, Binders, Printing Parameters, Equipment, and Post-Treatment," Ceram. Int., **45**(10), pp. 12609–12624.

[3] Mostafaei, A., Elliott, A. M., Barnes, J. E., Li, F., Tan, W., Cramer, C. L., Nandwana, P., and Chmielus, M., 2021, "Binder Jet 3D Printing—Process Parameters, Materials, Properties, Modeling, and Challenges," Prog. Mater. Sci., **119**, p. 100707.

[4] Li, M., Du, W., Elwany, A., Pei, Z., and Ma, C., 2020, "Metal Binder Jetting Additive Manufacturing: A Literature Review," ASME J. Manuf. Sci. Eng., **142**(9), p. 090801.

[5] Du, W., Ren, X., Ma, C., and Pei, Z., 2020, "Ceramic Binder Jetting Additive Manufacturing: A Literature Review on Density," ASME J. Manuf. Sci. Eng., **142**(4), p. 040801.

[6] Gonzalez, J., Mireles, J., Lin, Y., and Wicker, R., 2016, "Characterization of Ceramic Components Fabricated Using Binder Jetting Additive Manufacturing Technology," Ceram. Int., **42**(9), pp. 10559–10564.

[7] Mariani, M., Beltrami, R., Brusa, P., Galassi, C., Ardito, R., and Lecis, N., 2021, "3D Printing of Fine Alumina Powders by Binder Jetting," J. Eur. Ceram. Soc., **41**(10), pp. 5307–5315.

[8] Rishmawi, I., and Vlasea, M., 2021, "Binder Jetting of Silicon Steel, Part I: Process Map of Green Density," ASME J. Manuf. Sci. Eng., **143**(11), p. 111010.

[9] Vlasea, M., Shanbhag, G., and Wheat, E., 2020, "The Master Sinter Curve and Its Application to Binder Jetting Additive Manufacturing," ASME J. Manuf. Sci. Eng., **142**(10), p. 101002.

[10] Miao, G., Du, W., Moghadasi, M., Pei, Z., and Ma, C., 2020, "Ceramic Binder Jetting Additive Manufacturing: Effects of Granulation on Properties of Feedstock Powder and Printed and Sintered Parts," Addit. Manuf., **36**, p. 101542.

[11] Moghadasi, M., Du, W., Li, M., Pei, Z., and Ma, C., 2020, "Ceramic Binder Jetting Additive Manufacturing: Effects of Particle Size on Feedstock Powder and Final Part Properties," Ceram. Int., **46**(10), pp. 16966–16972.

[12] Du, W., Roa, J., Hong, J., Liu, Y., Pei, Z., and Ma, C., 2021, "Binder Jetting Additive Manufacturing: Effect of Particle Size Distribution on Density," ASME J. Manuf. Sci. Eng., **143**(9), p. 091002.

[13] Li, M., Miao, G., Moghadasi, M., Pei, Z., and Ma, C., 2021, "Ceramic Binder Jetting Additive Manufacturing: Relationships Among Powder Properties, Feed Region Density, and Powder Bed Density," Ceram. Int., **47**(17), pp. 25147–25151.

[14] Fine Ceramics, 2020, "Advanced Ceramics, Advanced Technical Ceramics—Determination of Density and Apparent Porosity," International Organization for Standardization (ISO 18754:2020).